Inorganica Chimica Acta, *198–200* (1992) 593–600

Synthesis of complexes with molybdenum–platinum bonds from the alkylidyne(carborane)molybdenum reagent $[NEt_4][Mo(\equiv CC_6H_4Me\text{-}4)(CO)_2(\eta^5\text{-}C_2B_9H_9Me_2)]$*

John C. Jeffery, Mark D. Mortimer and F. Gordon A. Stone**
School of Chemistry, The University, Bristol BS8 1TS (UK)

Abstract

Treatment of $[\textit{trans}\text{-PtH(Cl)(PEt}_3)_2]$, in tetrahydrofuran at −30 °C, with $[NEt_4][Mo(\equiv CC_6H_4Me\text{-}4)(CO)_2(\eta^5\text{-}C_2B_9H_9Me_2)]$, in the presence of $TlBF_4$, affords the thermally labile complex $[MoPt(CO)_2(PEt_3)_2\{\eta^6\text{-}C_2B_9H_8(CH_2C_6H_4Me\text{-}4)Me_2\}]$. Addition of donor molecules L [CO, PEt_3 or dppm ($Ph_2PCH_2PPh_2$)] to the latter at low temperatures yields the stable compounds $[MoPt(\mu\text{-}H)\{\mu\text{-}\sigma{:}\eta^5\text{-}C_2B_9H_7(CH_2C_6H_4Me\text{-}4)Me_2\}(CO)_2(L)(PEt_3)_2]$. The reaction between $[\textit{cis}\text{-PtCl(Me)(PMe}_2\text{Ph)}_2]$ and $[NEt_4][Mo(\equiv CC_6H_4Me\text{-}4)(CO)_2(\eta^5\text{-}C_2B_9H_9Me_2)]$ in tetrahydrofuran, in the presence of $TlBF_4$, gives a mixture of the dimetal compounds $[MoPt(\mu\text{-}CC_6H_4Me\text{-}4)(\mu\text{-}\sigma{:}\eta^5\text{-}C_2B_9H_8Me_2)(PMe_2Ph)]$ and $[MoPt(\mu\text{-}CC_6H_4Me\text{-}4)(\mu\text{-}\sigma{:}\eta^5\text{-}C_2B_9H_8Me_2)(CO)_2(PMe_2Ph)_2]$, from which the latter may be isolated pure by addition of PMe_2Ph. The NMR spectra (^1H, $^{13}C\{^1H\}$, $^{11}B\{^1H\}$ and $^{31}P\{^1H\}$) of the new complexes are reported and discussed in relation to the structures proposed.

Introduction

Salts of the anionic tungsten complexes $[W\equiv CR)(CO)_2(\eta^5\text{-}7,8\text{-}C_2B_9H_9R'_2]^-$ (R = alkyl, aryl or alkynyl; R′ = Me or H)† are versatile reagents for the synthesis of polynuclear metal complexes containing tungsten since they react with a great variety of low valent metal compounds. The products isolated often have novel molecular structures resulting from the non-spectator role displayed by the carborane cage ligands in these reactions [1, 2]. This feature provides an important impetus for further work in this area. So far relatively little has been done to extend this chemistry to anionic alkylidyne(carborane)molybdenum species, apart from a study of some reactions of $[NEt_4][Mo(\equiv CC_6H_4Me\text{-}4)(CO)\{P(OMe)_3\}(\eta^5\text{-}C_2B_9H_9Me_2)]$ leading to products with molybdenum–gold, –rhodium and –iron bonds [3]. Recently we have synthesized the salt $[NEt_4][Mo(\equiv CC_6H_4Me\text{-}4)(CO)_2(\eta^5\text{-}C_2B_9H_9Me_2)]$ (**1a**) and have shown that when treated with $HBF_4\cdot Et_2O$ in the presence of $[W(\equiv CMe)(CO)_2(\eta\text{-}C_5H_5)]$ the bimetal compound $[MoW(\mu\text{-}CMe)(CO)_3\{\eta^5\text{-}C_2B_9H_8(CH_2C_6H_4Me\text{-}4)Me_2\}(\eta\text{-}C_5H_5)]$ is obtained [4]. In this paper we report further reactions of **1a** in order to compare its reactivity towards certain platinum reagents with that of the analogous tungsten species **1b** and **1c**.

Results and discussion

Treatment of **1a** with $[\textit{trans}\text{-PtH(thf)(PEt}_3)_2][BF_4]$ (thf = tetrahydrofuran), prepared *in situ* by treating $[\textit{trans}\text{-PtCl(H)(PEt}_3)_2]$ with $TlBF_4$ in thf, gave an orange product **2a**, stable only below *c.* −30 °C. The spectroscopic data strongly support the formulation $[MoPt(CO)_2(PEt_3)_2\{\eta^6\text{-}C_2B_9H_8(CH_2C_6H_4Me\text{-}4)Me_2\}]$ for this species, a molybdenum analogue of the tungsten–platinum compound $[WPt(CO)_2(PEt_3)_2\{\eta^6\text{-}C_2B_9H_8(CH_2C_6H_4Me\text{-}4)Me_2\}]$ (**2b**) prepared in a similar manner from the salt **1b** and $[\textit{trans}\text{-PtH(thf)(PEt}_3)_2][BF_4]$ [5]. Compound **2b** is stable, and it was possible to establish its novel *hypercloso* structure by X-ray diffraction. In the IR spectrum it shows a single CO band at 1828 cm^{-1}, to be compared with

---

*This article is Part 114 of a series on the synthesis and structures of complexes containing bonds between different transition elements. For Part 113 see ref. 15.

**Author to whom correspondence should be addressed at the Department of Chemistry, Baylor University, Waco, TX 76798-7348, USA.

†In these anionic complexes a tungsten atom forms with a $[\textit{nido}\text{-}7,8\text{-}C_2B_9H_9R'_2]^{2-}$ anion a *closo*-1,2-dicarba-3-tungstadodecaborane icosahedral structure. However, in this and many of our other papers the carborane group is designated as $\eta^5\text{-}C_2B_9H_9R'_2$ in order to emphasise its pentahapto ligand properties in which it formally acts as a four-electron donor.

0020-1693/92/$5.00

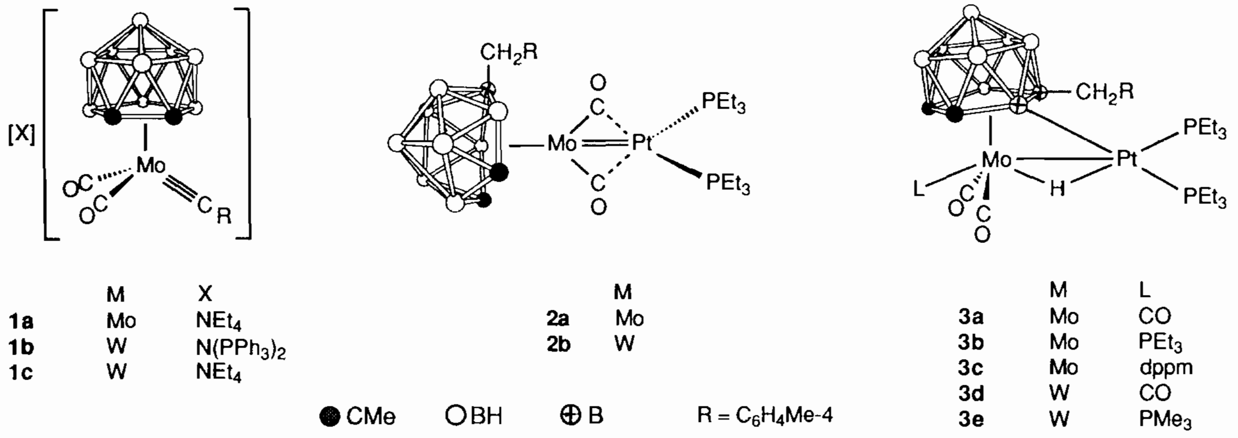

TABLE 1. Analytical[a] and other data for the molybdenum–platinum complexes

Compound[b]	Colour	Yield (%)	ν_{max}(CO)[c] (cm^{-1})	Analysis (%)	
				C	H
$[MoPt(CO)_2(PEt_3)_2\{\eta^6\text{-}C_2B_9H_8(CH_2R)Me_2\}]$[d] (**2a**)	orange		1835		
$[MoPt(\mu\text{-}H)\{\mu\text{-}\sigma\text{:}\eta^5\text{-}C_2B_9H_7(CH_2R)Me_2\}(CO)_3(PEt_3)_2]$ (**3a**)	orange	66	2016s 1952m 1910s	37.3(37.0)	6.4(6.1)
$[MoPt(\mu\text{-}H)\{\mu\text{-}\sigma\text{:}\eta^5\text{-}C_2B_9H_7(CH_2R)Me_2\}(CO)_2(PEt_3)_3]$ (**3b**)	orange	65	1920m 1833s	39.7(39.8)	7.4(7.1)
$[MoPt(\mu\text{-}H)\{\mu\text{-}\sigma\text{:}\eta^5\text{-}C_2B_9H_7(CH_2R)Me_2\}(CO)_2(PEt_3)_2(dppm)]$ (**3c**)	orange	38	1925m 1840s	[e]47.5(47.4)	6.5(5.9)
$[MoPt(\mu\text{-}H)\{\mu\text{-}\sigma\text{:}\eta^5\text{-}C_2B_9H_7(CH_2R)Me_2\}(CO)_2(PEt_3)_2]$ (**4**)	green	19	1925s 1858m	[e]34.9(34.8)	6.5(5.9)
$[MoPt(\mu\text{-}CR)(\mu\text{-}\sigma\text{:}\eta^5\text{-}C_2B_9H_8Me_2)(CO)_3(PMe_2Ph)]$[f] (**5a**)	red	40	2055m 2002s 1939s		
$[MoPt(\mu\text{-}CR)(\mu\text{-}\sigma\text{:}\eta^5\text{-}C_2B_9H_8Me_2)(CO)_2(PMe_2Ph)_2]$ (**5b**)	red	10	1982s 1913s	41.1(40.7)	5.7(4.9)

[a]Calculated values in parentheses. [b]R = C_6H_4Me-4. [c]Measured in CH_2Cl_2; a broad band is observed in all the spectra near 2550 cm^{-1} due to ν(BH). [d]Unstable, see text. [e]Crystallises with one molecule of CH_2Cl_2. [f]Inseparable mixture with **5b** (see text), microanalytical data not obtained.

that observed for **2a** at 1835 cm^{-1} (Table 1). The $^{31}P\{^1H\}$ NMR spectra are also similar. For **2a**, measured at −50 °C, there is a singlet at δ 37.2 ppm, with J(PtP) 3520 Hz. The corresponding data for **2b** are δ 35.7 ppm (J(PtP) 3347 Hz) [5].

A possible pathway for the formation of compound **2a** is shown on Scheme 1. There are several precedents for the $\mu\text{-}\sigma\text{:}\eta^3\text{-}C(H)C_6H_4Me$-4 ligand present in the proposed intermediate **A**, which would arise by addition of Pt–H to the C≡Mo bond [6, 7]. Intermediate **B** contains the well defined B–H⇀Pt bridge system [5, 8], and a terminal alkylidene group on the molybdenum. The final step to give **2a** involves the well established insertion of the alkylidene group into the cage B–H bond [4, 9], with cleavage of the cage C–C connectivity.

Compound **2a** is an electronically unsaturated 30 electron dimetal species. Accordingly treatment of its solutions in thf at −30 °C with donor molecules (L = CO, PEt_3 or dppm (diphenylphosphinomethane)) affords the complexes $[MoPt(\mu\text{-}H)\{\mu\text{-}\sigma\text{:}\eta^5\text{-}C_2B_9H_7(CH_2C_6H_4Me\text{-}4)Me_2\}(CO)_2(L)(PEt_3)_2]$ (**3a**, L = CO; **3b**, L = PEt_3; **3c**, L = dppm), data for which are given in Tables 1–3. The reactivity of **2a** towards donor molecules parallels that of **2b**, which with CO and PMe_3 yields the complexes **3d** and **3e**, respectively. In the compounds **3**, the carborane group has regained the *closo* icosahedral geometry, but a hydrogen atom from one of the BH groups in the *nido* face of the cage has migrated to bridge the metal–metal bond, with concomitant formation of an *exo*-polyhedral B–Pt σ bond.

The NMR data for the compounds **3a**–**3c** (Tables 2 and 3) are in complete agreement with the structures shown. In the ^1H NMR spectrum there are diagnostic resonances for the μ-H nuclei at δ −7.95 (**3a**), −8.60 (**3b**) and −8.54 (**3c**) each signal displaying coupling with non-equivalent ^{31}P nuclei. In the spectra of **3d** and **3e** the corresponding signals are at δ −8.81 and −8.45, respectively [5]. Peaks for the two diastereotopic protons of the BCH_2 group should occur as an AB pattern. In practice, one-half of this pattern is obscured by resonances due to the CH_2P nuclei. However, for **3a**–**3c** a broad doublet corresponding to one proton of the BCH_2 fragment is seen at δ 2.42 (**3a**), 2.63 (**3b**) and 2.59 (**3c**), with J(HH) c. 14 Hz. The BCH_2 group

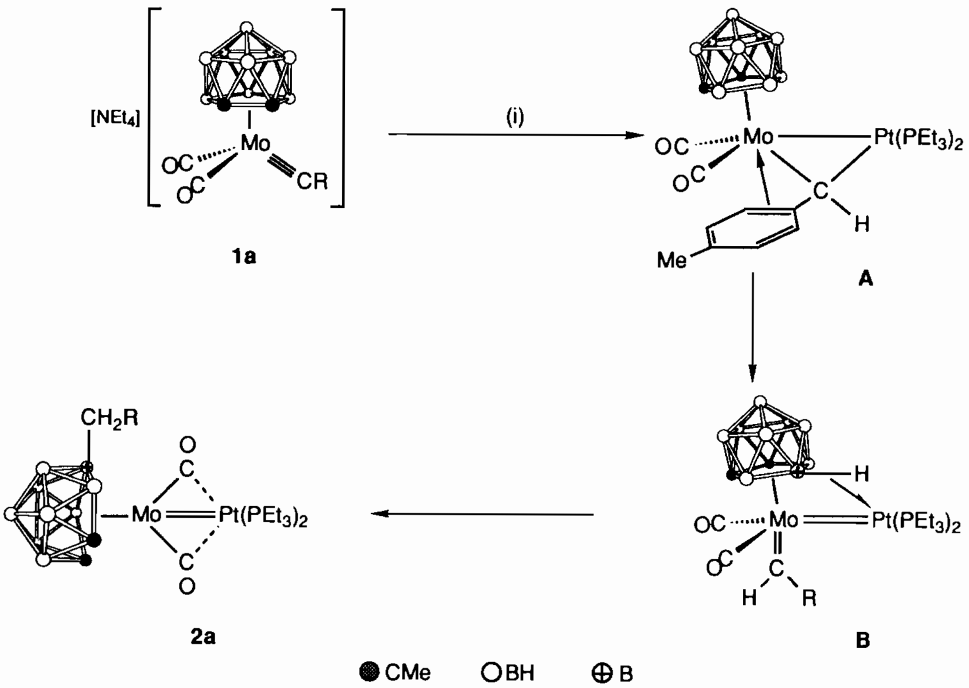

Scheme 1. R = C_6H_4Me-4, (i) + $[PtH(thf)(PEt_3)_2][BF_4]$.

in **3d** displays a similar pattern, with the resonance for one proton overlapping with that for the CH_2P nuclei, while the other signal appears at δ 2.47 ppm as a broad doublet (J(HH) 13 Hz) [5].

The CMe groups of the carborane cage are asymmetric in the compounds **3a**–**3c**, a feature displayed most clearly in the $^{13}C\{^1H\}$ NMR spectra. Thus for **3a** signals at δ 71.8 and 69.7 ppm (J(PtC) 39) may be assigned to the *C*Me nuclei, and those at 35.8 (J(PtC) 38) and 32.2 ppm to the C*Me* groups. Interestingly, ^{195}Pt–^{13}C couplings are observed on the peaks of one C*Me* and one *C*Me fragment. It is probable that these groups are α and β to the boron forming the B–Pt σ bond, respectively, leading to the observation of appreciable ^3J(PtC) couplings. The magnitude of such couplings vary in the sequence $^3J(PtC) > {}^2J(PtC) > {}^4J(PtC) \approx 0$ Hz [11].

The presence of the BCH_2 and BPt groups in the complexes **3a**–**3c** is fully confirmed by the $^{11}B\{^1H\}$ NMR spectra (Table 3). In each spectrum there are two relatively deshielded resonances, each corresponding in intensity to one boron nucleus. None of these resonances show ^1H–^{11}B coupling in the ^{11}B spectra, establishing that they are not due to BH groups. The more deshielded resonance in each pair may be ascribed to the BPt moieties. This signal is seen at δ 51.4, 39.6 and 40.2 ppm for **3a**, **3b** and **3c**, respectively, and for **3a** and **3b** the spectra were sufficiently well resolved for ^{11}B–^{195}Pt coupling to be observed: 550 Hz for **3a** and 450 Hz for **3b**. The second deshielded signal in each spectrum is due to the BCH_2 groups, and these are seen at δ 16.4 (**3a**), 13.1 (**3b**) and 13.8 ppm (**3c**). The $^{11}B\{^1H\}$ NMR data for **3e**, the structure of which has been established by X-ray diffraction, are very similar with resonances at δ 36.2 (BPt, J(PtB) 400 Hz) and 10.6 ppm (BCH_2).

The $^{31}P\{^1H\}$ NMR spectra (Table 3) are as expected. That for **3a** consists of a doublet signal at δ 24.4(J(PP) 18, J(PtP) 4082) and a broad peak at δ 14.2 ppm (J(PtP) 1740 Hz). The latter resonance may be assigned to the PEt_3 ligand *transoid* to the BPt group, the broadening being due to ^{11}B–^{31}P coupling. The former signal must thus be due to the PEt_3 ligand *transoid* to the Mo–Pt bond, and this is in agreement with the larger ^{195}Pt–^{31}P coupling observed for this resonance. The spectrum of **3b** displays three resonances. The apparent triplet at δ 28.8 ppm (J(PP) 8 and 6, J(PtP) 32 Hz) may be assigned to the $MoPEt_3$ fragment, and the signals at δ 25.2 (J(PP) 14 and 8, J(PtP) 4229) and 14.6 ppm (br, J(PtP) 1750 Hz) to the *cis*-$Pt(PEt_3)_2$ fragment. As would be anticipated, the $^{31}P\{^1H\}$ NMR spectrum of **3c** shows four resonances, these occurring at δ 47.7, 25.2, 16.4(br) and −28.1 ppm. The latter signal is diagnostic for the non-ligating PPh_2 group of the dppm molecule [10]. Indeed, the chemical shift is close to that (δ −23.1 ppm) for the free ligand, measured under the same conditions. The peaks at δ 16.4 and 25.2 ppm are due to the *cis*-$Pt(PEt_3)_2$ fragment, the broadness of the former signal resulting from *transoid* ^{11}B–Pt–^{31}P coupling. The fourth peak at δ 47.7 ppm, also broad, may be assigned to the $MoPPh_2$ moiety.

Compound **3c** was refluxed in thf in an attempt to displace a PEt_3 ligand, and induce formation of a

TABLE 2. ^{1}H and ^{13}C{^{1}H} NMR data[a] for the molybdenum–platinum complexes

Compound	^{1}H (δ)[b]	^{13}C{^{1}H} (δ)[c]
3a	−7.95 (d of d, 1 H, μ-H, *J*(PH) 51 and 16, *J*(PtH) 382), 1.05–1.19 (m, 18 H, $CH_2\mathit{Me}$), 2.05–2.21 (m, 13 H, CH_2Me and BCH_2), 2.02, 2.14, 2.24 (s×3, 9 H, CMe, Me-4), 2.42 (d, br, 1 H, BCH_2, *J*(HH) 13), 6.87, 6.92 ($(AB)_2$, 4 H, C_6H_4, *J*(AB) 8)	231.9 (CO), 227.0 (CO, *J*(PtC) 24), 224.5 (CO), 144.3 ($C^1(C_6H_4)$), 132.6, 129.3, 128.1 (C_6H_4), 71.8 (*C*Me), 69.7 (*C*Me, *J*(PtC) 39), 35.8 (C*Me*, *J*(PtC) 38), 34.0 (br, BCH_2), 32.2 (C*Me*), 21.0 (Me-4), 20.1, 17.9 (m×2, $\mathit{C}H_2Me$), 9.0, 8.6 (m×2, $CH_2\mathit{Me}$)
3b	−8.60 (d of d of d, 1 H, μ-H, *J*(PH) 54, 14, and 9, *J*(PtH) 443), 1.10 (m, 27 H, $CH_2\mathit{Me}$), 1.99 (m, 19 H, CH_2Me and BCH_2), 2.06, 2.10, 2.23 (s×3, 9 H, CMe and Me-4), 2.63 (d, br, 1 H BCH_2, *J*(HH) 14), 6.77, 6.89 ($(AB)_2$, 4 H, C_6H_4, *J*(AB) 8)	240.0 (d, CO, *J*(PC) 23), 234.6 (d, CO, *J*(PC) 30), 146.6 ($C^1(C_6H_4)$), 132.1, 128.9, 128.0 (C_6H_4), 66.3 (*C*Me), 66.2 (*C*Me, *J*(PtC) 38), 37.4 (C*Me*, *J*(PtC) 44), 32.9 (br, BCH_2), 30.5 (C*Me*), 21.0 (Me-4), 20.1, 17.7 (m×2, $\mathit{C}H_2Me$), 9.1, 8.5 (m×2, $CH_2\mathit{Me}$)
3c	−8.54 (d of d of d, 1 H, μ-H, *J*(PH) 53, 14, and 9, *J*(PtH) 431), 1.18 (m, 18 H, $CH_2\mathit{Me}$), 2.01 (s, 3 H, Me-4 or CMe), 2.15 (m, 13 H, CH_2Me and BCH_2), 2.21 (s, 6 H, Me-4 and/or CMe), 2.59 (d, br, 1 H, BCH_2, *J*(HH) 14), 3.65 (m, 2 H, PCH_2P), 6.42, 6.75 ($(AB)_2$, 4 H, C_6H_4, *J*(AB) 8), 6.88–7.95 (m, 20 H, Ph)	239.4 (d, CO, *J*(PC) 25), 236.5 (d, CO, *J*(PC) 31), 146.3 ($C^1(C_6H_4)$), 140.2–127.9 (C_6H_4 and Ph), 67.4 (*C*Me), 66.2 (*C*Me, *J*(PtC) 43), 37.3 (C*Me*. *J*(PtC) 44), 33.5 (br, BCH_2), 29.0 (d of d, PCH_2P, *J*(PC) 39 and 19), 27.8 (C*Me*), 21.0 (Me-4), 20.1, 17.6 (m×2, $\mathit{C}H_2Me$), 9.1, 8.6 (m×2, $CH_2\mathit{Me}$)
4	−4.50 (d of d, 1 H, μ-H, *J*(PH) 65 and 17, *J*(PtH) 470), 0.98 (m, 18 H, $CH_2\mathit{Me}$), 1.09, 2.24, 2.53 (s×3, 9 H, CMe and Me-4), 1.95–2.17 (m, 13 H, CH_2Me and BCH_2), 3.03 (d, br, 1 H, BCH_2, *J*(HH) 13), 6.86, 6.91 ($(AB)_2$, 4 H, C_6H_4, *J*(AB) 8)	255.4 (CO), 145.5 ($C^1(C_6H_4)$), 132.6, 129.0, 128.2 (C_6H_4), 74.4 (*C*Me), 70.6 (d, *C*Me, *J*(PC) 8), 37.6 (br, BCH_2), 31.1, 29.5 (C*Me*), 21.1 (Me-4), 20.8 (d, $\mathit{C}H_2Me$, *J*(PC) 22), 17.9 (d of d, $\mathit{C}H_2Me$, *J*(PC) 29 and 5, *J*(PtC) 73), 8.9, 8.7 ($CH_2\mathit{Me}$)
5a[d]	1.61 (d, 6 H, MeP, *J*(PH) 9, *J*(PtH) 20), 2.03 (s, 6 H, CMe), 2.36 (s, 3 H, Me-4), 6.55, 6.88 ($(AB)_2$, 4 H, C_6H_4, *J*(AB) 8), 7.19–7.46 (m, 5 H, Ph)	303.7 (μ-C), 219.9 (CO), 188.5 (d, CO, *J*(PC) 8, *J*(PtC) 1514), 149.8 (d, $C^1(C_6H_4)$, *J*(PC) 8), 136.2–121.6 (C_6H_4 and Ph), 62.6 (*C*Me), 27.6 (C*Me*), 19.0 (Me-4), 13.1 (d, MeP, *J*(PC) 32, *J*(PtC) 34)
5b	0.87 (d, 6 H, MeP, *J*(PH) 9, *J*(PtH) 20), 1.57 (d, 6 H, MeP, *J*(PH) 11, *J*(PtH) 38) , 2.08 (s, 6 H, CMe), 2.41 (s, 3 H, Me-4), 7.03–7.41 (m, 14 H, C_6H_4 and Ph)	[e]306.8 (d, μ-C, *J*(PC) 46), 227.0 (CO), 151.7 (d, $C^1(C_6H_4)$, *J*(PC) 7), 140.1–128.5 (C_6H_4 and Ph), 63.7 (*C*Me), 30.3 (C*Me*), 21.5 (Me-4), 16.8 (d, MeP, *J*(PC) 36, *J*(PtC) 49), 14.3 (d, MeP, *J*(PC) 22, *J*(PtC) 18)

[a] Chemical shifts (δ) in ppm, coupling constants in Hz. [b] Measured in CD_2Cl_2. Signals for BH groups occur as broad unresolved peaks in the range 0–3 ppm. [c] Hydrogen-1 decoupled, chemical shifts are positive to high frequency of $SiMe_4$, with measurements in CD_2Cl_2–CH_2Cl_2 unless otherwise stated. [d] Measurements made from a mixture with **5b**. [e] Measured in CD_2Cl_2/thf (1:1).

TABLE 3. ^{11}B{^{1}H} and ^{31}P{^{1}H} NMR data[a] for the molybdenum–platinum compounds

Compound	^{11}B{^{1}H} (δ)[b]	^{31}P{^{1}H} (δ)[c]
3a	51.4 (1 B, BPt, *J*(PtB) *c.* 550), 16.4 (1 B, BCH_2), 2.6 (1 B), −7.8 (3 B), −11.1 (2 B), −15.1 (1 B)	24.4 (d, *J*(PP) 18, *J*(PtP) 4082), 14.2 (br, *J*(PtP) *c.* 1740)
3b	39.6 (1 B, BPt, *J*(PtB) *c.* 450), 13.1 (1 B, BCH_2), −2.3 (1 B), −10.1 (3 B), −11.9 (2 B), −16.4 (1 B)	28.8 (app. t, $MoPEt_3$, *J*(PP) 8 and 6, *J*(PtP) 32), 25.2 (d of d, PEt_3, *J*(PP) 14 and 8, *J*(PtP) 4229), 14.6 (br, PEt_3, *J*(PtP) *c.* 1750)
3c	40.2 (1 B, BPt), 13.8 (1 B, BCH_2), −1.8 (1 B), −9.9 (5 B), −16.3 (1 B)	47.7 (br, $Mo\mathit{P}Ph_2CH_2PPh_2$), 25.2 (d of d, PEt_3, *J*(PP) 14 and 6, *J*(PtP) 4224), 16.4 (br, PEt_3, *J*(PtP) *c.* 1730), −28.1 (d, $MoPPh_2CH_2\mathit{P}Ph_2$, *J*(PP) 10)
4	41.8 (1 B, BPt), 25.6 (1 B, BCH_2), 2.1 (1 B), −3.5 (2 B), −7.7 (1 B), −10.0 (2 B), −12.6 (1 B)	20.7 (d, PEt_3, *J*(PP) 18, *J*(PtP) 3833), 15.7 (br, PEt_3, *J*(PtP) *c.* 1800)
5a[d]	54.1 (1 B, BPt), −6.8 to −18.0 (br, 8 B)	[e]−5.6 (br, *J*(PtP) *c.* 2700)
5b	52.7 (d, 1 B, *J*(PP) 64, *J*(PtP) 436), −8.5 to −17.2 (br, 8 B)	−0.4 (d, *J*(PP) 26, *J*(PtP) 3496), −6.9 (br, *J*(PtP) *c.* 2480)

[a] Chemical shifts (δ) in ppm, coupling constants in Hz, measurements in CD_2Cl_2 at ambient temperatures unless otherwise stated. [b] Hydrogen-1 decoupled, chemical shifts are positive to high frequency of $BF_3\cdot Et_2O$ (external). [c] Hydrogen-1 decoupled, chemical shifts are positive to high frequency of 85% H_3PO_4 (external). [d] ^{195}Pt{^{1}H} NMR (in CD_2Cl_2): δ −245 (d of q, *J*(PPt) *c.* 2700, *J*(BPt) *c.* 350); chemical shifts are to high frequency of $\Xi(^{195}Pt) = 21.4$ MHz. [e] Measured in $(CD_3)_2CO$/thf (1:1).

bridging μ-dppm group. However, this procedure was not successful, although formation of a pale green very insoluble species was observed which could not be characterised. Probably the dppm groups engage in intermolecular bridging, a process which might well lead to an insoluble product.

It was observed that if solutions of **2a** were allowed to warm above −30 °C, or if the reaction between **1a** and [PtH(thf)(PEt$_3$)$_2$][BF$_4$] was performed at room temperature, a mixture of products was obtained. Chromatography on alumina yielded a mixture of **3a** and **3b**, in a ratio of *c*. 4:1, which proved inseparable on the column. A subsequent green eluate afforded a product **4**, the formulation of which has not been fully resolved. Unfortunately, despite persistent efforts, crystals for an X-ray diffraction study could not be obtained. Nevertheless, there is good spectroscopic evidence (Tables 1–3) that **4** is the dimetal complex [MoPt(μ-H){μ-σ:η^5-C$_2$B$_9$H$_7$(CH$_2$C$_6$H$_4$Me-4)Me$_2$}(CO)$_2$(PEt$_3$)$_2$].

The ^{1}H NMR spectrum (Table 2) displays a resonance characteristic for a μ-H group at δ −4.50 which is a doublet of doublets, due to coupling with the non-equivalent PEt$_3$ ligands (*J*(PH) 65 and 17 Hz). The ^{195}Pt–^{1}H coupling of 470 Hz is also diagnostic for a hydrido ligand bridging a metal–metal bond involving platinum. The ^{1}H NMR reveals a broad doublet at δ 3.03 (*J*(HH) 13 Hz), corresponding to one half of the AB pattern produced by the diastereotopic protons of the BCH$_2$ group. As with the compounds **3**, the other half of this pattern is obscured by the PEt$_3$ resonances. The ^{11}B{^{1}H} NMR spectrum (Table 3) shows resonances with intensities corresponding to single boron nuclei at δ 41.8 and at 25.6 ppm, and these shifts are fully diagnostic for BPt and BCH$_2$ groups, respectively [5]. The ^{31}P{^{1}H} NMR spectrum (Table 3) shows two resonances with ^{31}P–^{31}P and ^{195}Pt–^{31}P couplings similar to those for the *cis*-Pt(PEt$_3$)$_2$ group in **3a**.

The IR spectrum reveals two CO stretching bands at 1925s and 1858s cm^{-1}. The latter frequency suggests a semi-bridging arrangement, leaving open the precise arrangement of the carbonyls. There is apparently a dynamic process which site-exchanges the CO ligands, since the ^{13}C{^{1}H} NMR spectrum displays only one CO resonance at δ 255.4. The relative peak intensity of this resonance when compared with that for the C^1(C$_6$H$_4$) nucleus suggests that the carbonyl signal is due to two CO ligands. Moreover, the chemical shifts is unusually deshielded for two terminal groups, but might be explained if a terminal and a bridging CO ligand were undergoing site exchange. The cage ligand is seen to be asymmetric by the presence in the ^{13}C{^{1}H} NMR spectrum of signals at δ 74.4 and 70.6 ppm (*C*Me) and 31.1 and 29.5 ppm (C*Me*) due to non-equivalent CMe groups. It is interesting to note that unlike the compound **3** no ^{195}Pt–^{13}C coupling is seen on the peaks for the CMe groups, but the resonance at δ 70.6 ppm is a doublet, presumably due to ^{31}P–^{13}C coupling (8 Hz) with the PEt$_3$ ligand *transoid* to the B–Pt bond.

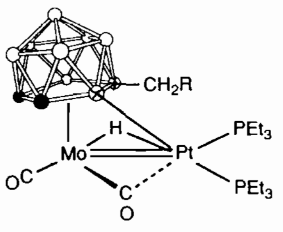

4

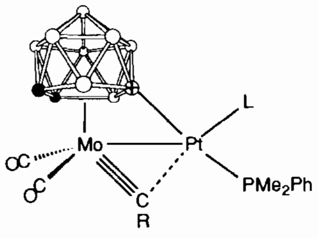

	M	L
5a	Mo	CO
5b	Mo	PMe$_2$Ph
5c	W	PMe$_2$Ph

● CMe ○ BH ⊕ B R = C$_6$H$_4$Me-4

Assuming the structure shown for **4** is correct, as seems likely based on the NMR data, its formation might arise through a thermally induced isomerisation of **2a** to relieve the electron deficiency of the *hypercloso*-cage. However, on present evidence assignment of the structure of **4** must remain somewhat tentative.

The reaction between **1a** and *cis*-[PtMe(thf)(PMe$_2$Ph)$_2$][BF$_4$] was next investigated. The latter species was prepared *in situ* by treating *cis*-[PtCl(Me)(PMe$_2$Ph)$_2$][BF$_4$] with TlBF$_4$, in thf at room temperature. Reaction with **1a** proceeds to afford a mixture of the two compounds [MoPt(μ-CC$_6$H$_4$Me-4)(μ-σ:η^5-C$_2$B$_9$H$_8$Me$_2$)(CO)$_3$(PMe$_2$Ph)] (**5a**) and [MoPt(μ-CC$_6$H$_4$Me-4)(μ-σ:η^5-C$_2$B$_9$H$_8$Me$_2$)(CO)$_2$(PMe$_2$Ph)$_2$] (**5b**) in the ratio 4:1. This mixture proved inseparable by chromatography. However, treatment of the product mixture with an excess of PMe$_2$Ph yielded pure **5b**. The latter is the molybdenum analogue of the complex [WPt(μ-CC$_6$H$_4$Me-4)(μ-σ:η^5-C$_2$B$_9$H$_8$Me$_2$)(CO)$_2$(PMe$_2$Ph)$_2$] (**5c**), the structure of which has been established by X-ray crystallography [12]. Compound **5c** was obtained by treating **1c** with [*cis*-PtMe(Me$_2$CO)(PMe$_2$Ph)$_2$][BF$_4$]. Interestingly, an isomer of **1c** was also formed in this reaction, having a structure in which the B–Pt σ bond involves a boron atom α to a carbon in the open pentagonal $\overline{\mathrm{CC}B\mathrm{BB}}$ face of the cage. There was no evidence for the formation of a similar isomer in the synthesis of **5b** for which, as described below, there is good NMR evidence for the presence of a B–Pt σ bond involving a boron in the β site of the $\overline{\mathrm{CCB}B\mathrm{B}}$ ring ligating the molybdenum.

Since **5b** could be isolated free of **5a**, it could be fully characterised by microanalysis and by its spectroscopic properties (Tables 1–3). The IR spectrum shows two IR stretching bands at 1982 and 1913 cm^{-1}, as well as the usual broad BH stretch for the carborane cage at 2552 cm^{-1}. The presence of the B–Pt σ bond is revealed in the $^{11}B\{^1H\}$ NMR spectrum by a doublet resonance at δ 52.7 ppm (J(PB) 64 Hz) with ^{195}Pt satellite peaks (J(PtB) 436 Hz). The $^{31}P\{^1H\}$ NMR spectrum displays a doublet resonance at δ -0.4 (J(PP) 26, J(PtP) 3496) and a broad signal at -6.9 ppm (J(PtP) 2480 Hz). The latter may be ascribed to the PMe_2Ph group *transoid* to the B–Pt σ bond. These $^{11}B\{^1H\}$ and $^{31}P\{^1H\}$ NMR data are very similar to those for **5c**: $^{11}B\{^1H\}$, δ 48.2 (d, BPt, J(PB) 68, J(PtB) 533); $^{31}P\{^1H\}$, δ -2.3 (d, J(PP) 25, J(PtP) 3607) and -5.2 ppm (br, J(PtP) 2500 Hz) [12].

In the $^{13}C\{^1H\}$ NMR spectrum of **5b** a doublet resonance is seen at δ 306.8 ppm (J(PC) 46 Hz) for the ligated carbon atom of the bridging alkylidyne ligand. The chemical shift is very close to that found for the C$\equiv$Mo nucleus in the precursor **1a** (δ 305.7 ppm). This indicates that in **5b**, as in **5c** (μ-C, δ 290.4 ppm, J(PC) 36 Hz), the alkylidyne group semi-bridges the W–Pt bond, lying much closer to the tungsten atom than to the platinum. The X-ray diffraction study of **5c** revealed a W–C distance of 1.89(1) Å and a Pt–C separation of 2.14(1) Å [12]. The W–C separation is similar to that observed for the C$\equiv$W bond (1.83(1) Å) in the mononuclear tungsten complex $[PPh_4][W(\equiv CC_6H_4Me\text{-}4)(CO)_2(\eta^5\text{-}C_2B_9H_9Me_2]$ [13].

It is evident from the $^{13}C\{^1H\}$ NMR spectrum of **5b** that the molecule has a plane of symmetry encompassing the two metal atoms, the μ-C atom, the B atom σ bonded to the platinum, and the mid-point of the connectivity between the cage carbon atoms. This leads to the carbonyl groups being in similar environments, and hence only one resonance is observed, at δ 227.0 ppm. Similarly only one signal is seen for the *C*Me and C*Me* nuclei, at δ 63.7 and 30.3 ppm, respectively. This information is supported by the ^1H NMR spectrum, which shows one peak for the CMe groups at δ 2.08 ppm.

Complex **5a**, the major component of the product mixture resulting from reaction of **1a** with [*cis*-$PtMe(thf)(PMe_2Ph)_2][BF_4]$, has three carbonyl stretching bands in the IR spectrum at 2055, 2002 and 1939 cm^{-1}. Two peaks are seen in the $^{13}C\{^1H\}$ NMR spectrum at δ 219.9 and 188.5 ppm. The latter is a doublet (J(PC) 8 Hz) with ^{195}Pt satellite peaks (J(PtP) 1514 Hz) and can be assigned to the PtCO group, whereas the former represents the two equivalent MoCO groups. The $^{31}P\{^1H\}$ NMR spectrum shows only one resonance (δ -5.6 ppm, J(PtP) 2700 Hz), and the broadness of the peak indicates that the phosphine is *transoid* to the B–Pt σ bond. The presence of the B–Pt linkage is indicated by a resonance in the $^{11}B\{^1H\}$ NMR spectrum at δ 54.1 ppm, showing shoulders due to ^{195}Pt coupling. The magnitude of this coupling can be estimated from the $^{195}Pt\{^1H\}$ NMR spectrum, which consists of a single resonance at δ -245 ppm split into a doublet of quartets (J(PPt) 2700, J(BPt) 350 Hz). As in **5b**, only two resonances are seen for the CMe groups in the $^{13}C\{^1H\}$ NMR spectrum (δ 62.6 (*C*Me) and 27.6 ppm (C*Me*)). Similarly, in the ^1H NMR spectrum only one peak is seen for the CMe groups at δ 2.03. The equivalence of the two MoCO ligands and the two CMe groups confirms that **5a** exists as the isomer with the β-boron of the CCB*B*B pentagonal ring forming the B–Pt bond. The alkylidyne carbon resonance, at δ 303.7 ppm in the $^{13}C\{^1H\}$ NMR spectrum, is in the semi-bridging region and shows neither ^{31}P nor ^{195}Pt coupling, being *cisoid* to the phosphine on the platinum centre. Interestingly, the C^1 atom of the C_6H_4 ring shows coupling to phosphorus (δ 149.8 ppm, J(PC) 8 Hz), presumably because it is a ^3J coupling. A similar feature is seen in the spectrum of **5b**. As **5a** was part of an inseparable mixture, microanalytical data were not forthcoming.

Scheme 2 shows a likely pathway for the formation of the complexes **5a** and **5b**. Intermediate **C** would result from displacement of a PMe_2Ph ligand from platinum as a result of forming a B–H$\rightharpoonup$Pt three-centre two-electron bond. This type of linkage has ample precedent, as has previously been mentioned [1, 5, 8]. The linkage may be viewed as incipient oxidative-addition of a B–H group at the Pt centre, and the next step would be reductive elimination releasing methane and forming **D**. Intermediate **C** is modelled on the compound $[WPtH(\mu\text{-}CC_6H_3Me_2\text{-}2,6)(CO)_2(PEt_3)(\eta^5\text{-}C_2B_9H_9Me_2)]$ which contains both a terminal Pt–H group and an exo-polyhedral B–H$\rightharpoonup$Pt linkage [8]. This hydrido tungsten–platinum complex slowly releases hydrogen gas yielding a mixture of $[WPt(\mu\text{-}CC_6H_3Me_2\text{-}2,6)(\mu\text{-}\sigma{:}\eta^5\text{-}C_2B_9H_8Me_2)(CO)_2(PEt_3)]$ and $[WPt(\mu\text{-}CC_6H_3Me_2\text{-}2,6)(\mu\text{-}\sigma{:}\eta^5\text{-}C_2B_9H_8Me_2)(CO)_3(PEt_3)]$ the structures of both of which have been determined by X-ray diffraction. Hence the suggested loss of methane in the formation of **D** is reasonable.

Intermediate **D** is similar to to the aforementioned species $[WPt(\mu\text{-}CC_6H_3Me_2\text{-}2,6)(\mu\text{-}\sigma{:}\eta^5\text{-}C_2B_9H_8Me_2)(CO)_2(PEt_3)]$, and with the Pt centre formally having only 14 valence electrons, it readily adds a CO molecule to give $[WPt(\mu\text{-}CC_6H_3Me_2\text{-}2,6)(\mu\text{-}\sigma{:}\eta^5\text{-}C_2B_9H_8Me_2)(CO)_3(PEt_3)]$. Likewise, intermediate **D** would also be expected to add a donor molecule to relieve the unsaturation of the platinum centre. The presence of free PMe_2Ph in solution would lead to **5b**, but the concomitant formation of **5a** is not surprising since CO is readily scavenged by metal centres in these types of reaction. Moreover, the relatively high proportion of **5a** formed, compared with **5b**, may well arise because the PMe_2Ph released in the initial step, would react with the reagent $[PtMe(thf)(PMe_2Ph)_2][BF_4]$ to yield the very stable cationic complex $[PtMe(PMe_2Ph)_3]^+$. Although this cation was not identified in the present study, it could have been present in the

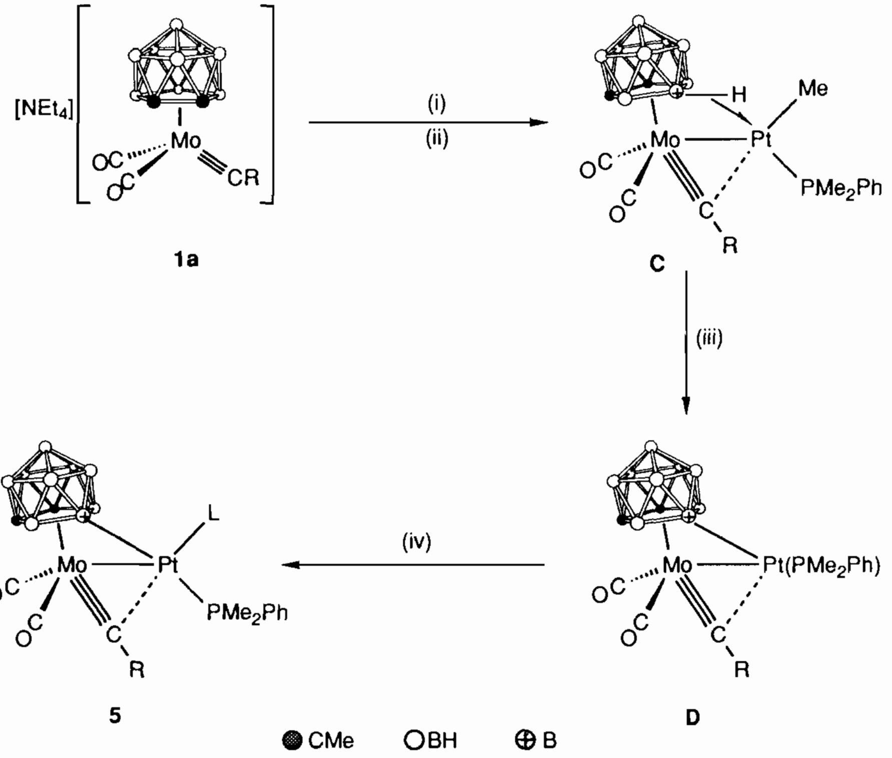

Scheme 2. R = C_6H_4Me-4, (i) +$[PtMe(thf)(PMe_2Ph)_2][BF_4]$, (ii) −$PMe_2Ph$, (iii) −$CH_4$, (iv) +L (CO or PMe_2Ph).

mixture, since it has been observed in the synthesis of **5c** [12].

Treatment of solutions of **5b** with CO gas results in the formation of **5a**. However, the reaction does not go to completion, presumably because of competition from the displaced PMe_2Ph for the coordination site on platinum. Upon removal of solvent *in vacuo* from the solutions, complex **5b** is regenerated quantitatively.

The new compounds described significantly extend the range of known species with molybdenum–platinum bonds [14]. Moreover, the presence of the exopolyhedral B–Pt σ bonds in the various products represents an interesting structural feature. Whilst the reactivity of the molybdenum salt **1a** towards the platinum reagents is generally similar to that of tungsten analogues **1b** or **1c**, differences are observed, as in the instability of **2a** versus **2b**, and in the formation of **5a**, the tungsten analogue of which is not formed in the synthesis of **5c** from [*cis*-$PtMe(Me_2CO)(PMe_2Ph)_2][BF_4]$.

Experimental

Experiments were carried out under nitrogen using Schlenk-tube techniques. All solvents were rigorously dried before use. Light petroleum refers to that fraction of b.p. 40–60 °C. Chromatography columns (*c*. 20 cm in length and 3 cm in diameter) were packed with alumina (Brockmann activity II). The IR spectra were measured with a Perkin-Elmer FT1600 spectrometer, and NMR spectra with JEOL JNM GX270 and GX400 instruments. The salt **1a** was prepared as previously reported [4], and the platinum reagents [*trans*-$PtH(thf)(PEt_3)_2][BF_4]$ and [*cis*-$PtMe(thf)(PMe_2Ph)_2]$-$[BF_4]$ were generated *in situ* as described below. Data characterising the new compounds are given in Tables 1–3.

Reactions of [NEt₄[Mo(≡CC₆H₄Me-4)(CO)₂(η⁵-C₂B₉H₉Me₂)] with [PtH(thf)(PEt₃)₂][BF₄]

The compound *trans*-$[PtH(Cl)(PEt_3)_2][BF_4]$ (0.08 g, 0.18 mmol), in thf (20 cm^3) at −30 °C, was treated with $TlBF_4$ (0.05 g, 0.18 mmol) and **1a** (0.10 g, 0.18 mmol), and the mixture was stirred for *c*. 2 h to yield an orange solution containing $[MoPt(CO)_2(PEt_3)_2\{\eta^6$-$C_2B_9H_8(CH_2C_6H_4Me\text{-}4)Me_2\}]$ (**2a**). Solutions of this species were stable below *c*. −30 °C, and were used without further purification.

(i) Carbon monoxide gas was bubbled through the solution of **2a** for 5 min, and then the mixture was allowed to warm to room temperature. Solvent was removed *in vacuo*, and the residue redissolved in CH_2Cl_2 (30 cm^3). The resulting suspension was filtered through a Celite plug (*c*. 2×1 cm), and the plug washed with CH_2Cl_2 (2×10 cm^3) with the washings being combined with the filtrate. The solution was evaporated to dryness *in vacuo*, redissolved in CH_2Cl_2–light petroleum (2 cm^3, 2:3) and chromatographed at room temperature. Elution with the same solvent mixture afforded an orange eluate, and removal of solvent *in vacuo* gave orange microcrystals of $[MoPt(\mu\text{-}H)\{\mu\text{-}\sigma{:}\eta^5\text{-}C_2B_9H_7(CH_2C_6H_4Me\text{-}4)Me_2\}(CO)_3(PEt_3)_2]$ (**3a**) (0.11 g).

(ii) In a similar manner, a solution of **2a** made from *trans*-$[PtH(Cl)(PEt_3)_2]$ (0.08 g, 0.18 mmol), $TlBF_4$ (0.05 g, 0.18 mmol) and **1a** (0.10 g, 0.18 mmol) was treated with PEt_3 (25 μl, 0.26 mmol) to give orange microcrystals of $[MoPt(\mu\text{-}H)\{\mu\text{-}\sigma{:}\eta^5\text{-}C_2B_9H_7(CH_2C_6H_4Me\text{-}4)Me_2\}(CO)_2(PEt_3)_3]$ (**3b**) (0.11 g).

(iii) A solution of **2a** made from *trans*-$[PtH(Cl)(PEt_3)_2]$ (0.10 g, 0.21 mmol), $TlBF_4$ (0.06 g, 0.20 mmol) and **1a** (0.11 g, 0.20 mmol) was treated with dppm (0.23 g, 0.60 mmol), in a similar manner to (i) above, to afford orange microcrystals of $[MoPt(\mu\text{-}H)\{\mu\text{-}\sigma{:}\eta^5\text{-}C_2B_9H_7(CH_2C_6H_4Me\text{-}4)Me_2\}(CO)_2(PEt_3)_2(dppm)]$ (**3c**) (0.10 g).

(iv) The compounds *trans*-$[PtH(Cl)(PEt_3)_2]$ (0.17 g, 0.36 mmol), $TlBF_4$ (0.13 g, 0.38 mmol) and **1a** (0.20 g, 0.36 mmol) were stirred together at room temperature in thf (20 cm^3) for 1 h. The solvent was removed *in vacuo*, and the residue redissolved in CH_2Cl_2 (50 cm^3). The resulting suspension was filtered through a Celite plug (*c*. 2×3 cm) to remove TlCl, and the plug washed with CH_2Cl_2 (2×15 cm^3), the washings being combined with the filtrate. The solution was reduced to an oil *in vacuo* and redissolved in CH_2Cl_2–light petroleum (6 cm^3, 2:3) and chromatographed. Elution with the same solvent mixture gave first an orange band comprising a mixture of **3a** and **3b** in approximately 4:1 proportion, followed by a green band. Solvent was removed from the green eluate *in vacuo*, and the residue dissolved in CH_2Cl_2 (1 cm^3). Addition of light petroleum (*c*. 5 cm^3) to the rapidly stirring solution afforded green microcrystals of $[MoPt(\mu\text{-}H)\{\mu\text{-}\sigma{:}\eta^5\text{-}C_2B_9H_7(CH_2C_6H_4Me\text{-}4)Me_2\}(CO)_2(PEt_3)_2]$ (**4**) (0.06 g).

Reactions of $[NEt_4][Mo(\equiv CC_6H_4Me\text{-}4)(CO)_2(\eta^5\text{-}C_2B_9H_9Me_2)]$ *with* $[PtMe(thf)(PEt_3)_2][BF_4]$

(i) A mixture of the compounds **1a** (0.21 g, 0.38 mmol), *cis*-$[PtCl(Me)(PMe_2Ph)_2]$ (0.20 g, 0.38 mmol) and $TlBF_4$ (0.15 g, 0.60 mmol) was stirred in thf (20 cm^3) at room temperature for 16 h. The suspension was allowed to settle, and the supernatant solution was decanted. The residue was washed with thf (2×5 cm^3) and the washings combined with the solution. Solvent was removed *in vacuo*, the residue redissolved in CH_2Cl_2 (6 cm^3), and the solution chromatographed. Elution with CH_2Cl_2 gave a dark red eluate. Removal of solvent *in vacuo* gave red microcrystals which were found to be a *c*. 4:1 mixture of $[MoPt(\mu\text{-}CC_6H_4Me\text{-}4)(\mu\text{-}\sigma{:}\eta^5\text{-}C_2B_9H_8Me_2)(CO)_3(PMe_2Ph)]$ (**5a**) and $[MoPt(\mu\text{-}CC_6H_4Me\text{-}4)(\mu\text{-}\sigma{:}\eta^5\text{-}C_2B_9H_8Me_2)(CO)_2(PMe_2Ph)_2]$ (**5b**) (0.16 g).

(ii) A mixture of **5a** and **5b** (0.10 g), prepared as described above, was treated with an excess of PMe_2Ph (0.20 cm^3) in CH_2Cl_2 (10 cm^3). Following gas evolution, the solvent was removed *in vacuo* and the residue was washed with light petroleum (3×15 cm^3) to yield red microcrystals of pure **5b** (0.11 g).

Acknowledgement

We thank the Science and Engineering Research Council for a research studentship (to M.D.M.).

References

1 F. G. A. Stone, *Adv. Organomet. Chem.*, *31* (1990) 53.

2 (a) J.-L. Cabioch, S. J. Dossett, I. J. Hart, M. U. Pilotti and F. G. A. Stone, *J. Chem. Soc., Dalton Trans.*, (1990) 519; (b) S. J. Dossett, I. J. Hart, M. U. Pilotti and F. G. A. Stone, *J. Chem. Soc., Dalton Trans.*, (1991) 511; (c) S. A. Brew and F. G. A. Stone, *J. Chem. Soc., Dalton Trans.*, (1992) 867.

3 D. D. Devore, C. Emmerich, J. A. K. Howard and F. G. A. Stone, *J. Chem. Soc., Dalton Trans.*, (1989) 797.

4 S. A. Brew, N. Carr, M. D. Mortimer and F. G. A. Stone, *J. Chem. Soc., Dalton Trans.*, (1991) 811.

5 M. J. Attfield, J. A. K. Howard, A. N. de M. Jelfs, C. M. Nunn and F. G. A. Stone, *J. Chem. Soc., Dalton Trans.*, (1987) 2219.

6 J. C. Jeffery, C. Sambale, M. F. Schmidt and F. G. A. Stone, *Organometallics*, *1* (1982) 1597; J. C. Jeffery, J. C. V. Laurie, I. Moore, H. Razay and F. G. A. Stone, *J. Chem. Soc., Dalton Trans.*, (1984) 1563; M. Green, J. A. K. Howard, A. N. de M. Jelfs, O. Johnson and F. G. A. Stone, *J. Chem. Soc., Dalton Trans.*, (1987) 73.

7 J. H. Davis and C. M. Lukehart, *Organometallics*, *3* (1984) 1763.

8 D. D. Devore, J. A. K. Howard, J. C. Jeffery, M. U. Pilotti and F. G. A. Stone, *J. Chem. Soc., Dalton Trans.*, (1989) 303.

9 S. A. Brew, D. D. Devore, P. D. Jenkins, M. U. Pilotti and F. G. A. Stone, *J. Chem. Soc., Dalton Trans.*, (1992) 393; N. Carr, J. C. Jeffery, M. U. Pilotti and F. G. A. Stone, *J. Am. Chem. Soc.*, (1991) in press; J. C. Jeffery, S. Li, D. W. I. Sams, and F. G. A. Stone, *J. Chem. Soc., Dalton Trans.*, (1992) 877.

10 K. A. Mead, I. Moore, F. G. A. Stone and P. Woodward, *J. Chem. Soc., Dalton Trans.*, (1983) 2083; M. R. Awang, J. C. Jeffery and F. G. A. Stone, *J. Chem. Soc., Dalton Trans.*, (1983) 2091.

11 J. Browning, P. L. Goggin, R. J. Goodfellow, N. W. Hurst, L. G. Mallinson and M. Murray, *J. Chem. Soc., Dalton Trans.*, (1978) 872.

12 N. Carr, M. C. Gimeno and F. G. A. Stone, *J. Chem. Soc., Dalton Trans.*, (1990) 2617.

13 O. Johnson, J. A. K. Howard, M. Kapan and G. M. Reisner, *J. Chem. Soc., Dalton Trans.*, (1988) 2903.

14 D. A. Roberts and G. L. Geoffroy, in G. Wilkinson, F. G. A. Stone and E. W. Abel (eds.), *Comprehensive Organometallic Chemistry*, Vol. 6, Pergamon, Oxford, 1982, pp. 763–877.

15 N. Carr, J. R. Fernandez and F. G. A. Stone, *Organometallics*, *114* (1992) 2203.